Journal of Great Lakes Research 49 (2023) 357–367

Contents lists available at ScienceDirect

Journal of Great Lakes Research

journal homepage: www.elsevier.com/locate/ijglr

Temporal changes in the remote sensing reflectance at Lake Vänern

Ilaria Cazzaniga [a,*], Giuseppe Zibordi [a], Krista Alikas [b], Susanne Kratzer [c]

[a] European Commission, Joint Research Centre (JRC), Ispra, Italy
[b] Tartu Observatory of the University of Tartu, Toravere, Estonia
[c] Department of Ecology, Environment and Plant Sciences (DEEP), Stockholm University, Stockholm, Sweden

ARTICLE INFO

Article history:
Received 22 June 2022
Accepted 12 January 2023
Available online 23 January 2023
Communicated by Caren Binding

Keywords:
Inland waters
Remote sensing reflectance
Earth observation
Trend analysis
Essential Climate Variables (ECV)
Climate change

ABSTRACT

The Aerosol Robotic Network - Ocean Color (AERONET-OC) instrument located at the Pålgrunden site in Lake Vänern provides values of remote sensing spectral reflectance $R_{RS}(\lambda)$ since 2008. These in situ $R_{RS}(\lambda)$ indicated a temporal increase from 2015 at center-wavelengths in the green and red spectral regions. To investigate the environmental and climate processes responsible for this increase, water color trends in Lake Vänern were analyzed considering in situ limnological measurements, meteo-climatic quantities and additionally satellite-derived data products from the Moderate Resolution Imaging Spectroradiometer on board the Aqua platform (MODIS-A). Satellite ocean color $R_{RS}(\lambda)$ data assessed against in situ $R_{RS}(\lambda)$ from the Pålgrunden site showed satisfactory agreement at a number of spectral bands. Relying on these validation results, comprehensive statistical analysis were performed using MODIS-A $R_{RS}(\lambda)$. These indicated periodical changes between 2002 and 2021 with clear minima occurring between 2010 and 2013. The complementary analyses of temporal changes characterizing limological and meteo-climatic quantities, and also relationships between these quantities and $R_{RS}(\lambda)$, indicated the existence of complex and concurrent bio-geochemical processes influencing water color in Lake Vänern. In particular, significant correlations were observed between $R_{RS}(\lambda)$ and *turbidity*, and also between $R_{RS}(\lambda)$ and total biovolume. Additionally, an early warming of Lake Vänern surface waters was identified since spring 2014. This occurrence could potentially affect the vertical mixing and water exchange between turbid coastal and pelagic waters with implications for phytoplankton phenology.

Introduction

The color of natural waters, which is usually investigated through water reflectance, provides invaluable information on their biogeochemical status and quality. Relying on this principle, since 2011 Lake Water Reflectance is listed amongst the Essential Climate Variables (ECV) as a direct indicator for biogeochemical processes and of the frequency of extreme events (ESA, 2021). This is supported by studies presenting the effects of climate change on lakes in terms of variation in water quality, trophic status, phytoplankton biomass and composition (e.g., Anderson, 2000; Hrycik et al., 2021; Whitehead et al., 2009 and references therein).

Over the last decades, several studies focusing on the variation of water color in boreal lakes showed alterations in the absorption coefficient of the dissolved organic matter at 420 nm $a_{CDOM}(420)$, which were explained by the impact of climate change in the northern hemisphere (see Weyhenmeyer et al., 2014 and references therein). For instance, brownification of Swedish surface waters was reported in several studies (de Wit et al., 2016; Johansson et al., 2010; Klante et al., 2021; Kritzberg, 2017; Kritzberg et al., 2020). In particular, Johansson et al. (2010) documented cyclic patterns for water color in Lake Mälaren due to the North Atlantic Oscillation (*NAO*) index. Brownification of Lake Bolmen in the south of Sweden was linked to short-term air temperature and precipitation variations (Klante et al., 2021). The temperature change was also shown to affect phytoplankton growth and composition (Weyhenmeyer, 2001; Weyhenmeyer et al., 2008; Yang et al., 2016). In the case of Lake Vänern, total phytoplankton biomass and phytoplankton composition were found to change significantly due to the occurrence of winter ice-cover (Weyhenmeyer et al., 2008).

The use of Earth observation technology to monitor inland waters, although still requiring consolidation, was already shown to be an invaluable tool complementing traditional field investigations (Tyler et al., 2016). Within such a general framework, the Ocean Color component of the Aerosol Robotic Network (AERONET-OC) contributes to lake water investigations by sup-

* Corresponding author.
E-mail address: Ilaria.Cazzaniga@ec.europa.eu (I. Cazzaniga).

https://doi.org/10.1016/j.jglr.2023.01.006
0380-1330/

porting local monitoring programs and the validation of satellite data products through automated in situ measurements of normalized water-leaving radiance $L_{WN}(\lambda)$ (Zibordi et al., 2021). With reference to the Pålgrunden AERONET-OC site operated at Lake Vänern (Sweden) since 2008, a temporal increase of $L_{WN}(\lambda)$ and of the derived remote sensing reflectance $R_{RS}(\lambda)$, has been observed during recent years at center-wavelengths in the green and red spectral regions. Concerned by such a finding, trends in $R_{RS}(\lambda)$ and time-series of bio-physical quantities in Lake Vänern were investigated by exploiting satellite-derived radiometric data products with the objective to identify those environmental and climate processes responsible for the increase in water reflectance. This was addressed by analyzing temporal trends and correlations between satellite radiometric data products and in situ time-series of limnological and meteo-climatic quantities.

Materials and methods

Study area

Lake Vänern is the largest lake in Sweden and the third largest in the European Union. It is on average 27 m deep with stratified waters in summer. Lake Vänern is divided by an archipelago extending in the North-South direction (Dahl and Pers, 2004), which naturally identifies two sub-basins characterized by cyclonic circulation and irregular wind-driven water exchanges. The contribution of direct precipitation on the lake with respect to the inflow from the catchment is about 25% (Larson, 2012). In spring, a thermal barrier of approximately 4 °C, responsible for the so-called thermal bar effect, builds up from the coast to the open lake region impacting pollution patterns and biological production. This phase is characterized by an intense vertical circulation of water (Kvarnäs, 2001).

Lake Vänern is considered oligotrophic because of its low phytoplankton biomass. Its water is generally classified as moderately nutrient-rich (Willén, 2001) and it is optically dominated by colored dissolved organic matter *CDOM* (Reinart et al., 2004; Philipson et al., 2016).

The whole lake basin was adversely affected by eutrophication in the 1960s and 1970s. Afterwards, the construction of wastewater treatment plants reduced the input of phosphorous and of oxygen consuming substances (Dahl and Pers, 2004). In addition, after years of steady increase, since 2019 the levels of organic matter in its tributary rivers stabilized, or even decreased (ESPON, 2021). Still, eutrophication locally affects some bays and the archipelago areas (Sandström et al., 2014).

In situ data

AERONET-OC is a network of globally distributed autonomous sun-photometers deployed on offshore fixed structures conceived to support ocean color activities (Zibordi et al., 2021, 2009b). It provides measurements of $L_{WN}(\lambda)$ and aerosol optical depth $\tau_a(\lambda)$ at various center-wavelengths λ in the visible and near-infrared spectral regions. Two different AERONET-OC instrument models have been operated at the Pålgrunden Lighthouse in Lake Vänern since 2008: CE-318 9-band radiometers from 2008 until 2018, and CE-318-T 12-band radiometers since 2019. This AERONET-OC site, called Pålgrunden, is located in the south-eastern part of the western basin close to the archipelago area (see Fig. 1) and is exclusively operated during ice-free months, typically from May through September. In this study, Level 2.0 normalized water-leaving radiance $L_{WN}(\lambda)$ data, corrected for bidirectional effects, were used to determine in situ $R_{RS}^{PRS}(\lambda)$ as:

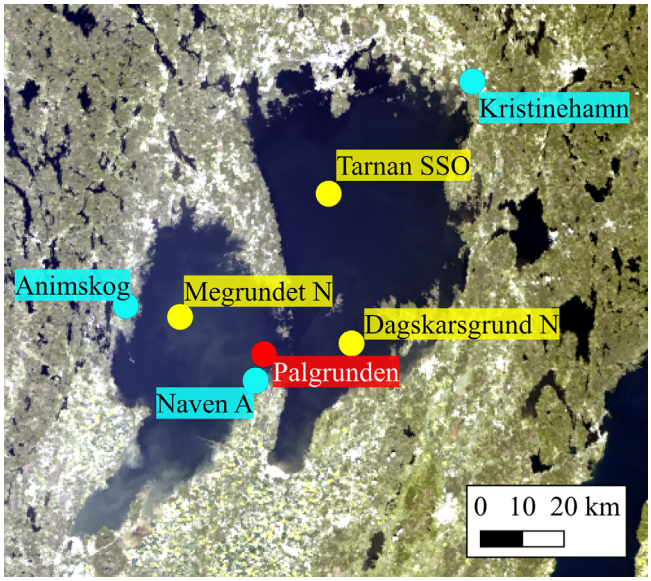

Fig. 1. Measurement locations relevant for this study: the Pålgrunden AERONET-OC site (in red); the meteorological stations Kristinehamn, Animskog, and Naven A (in cyan) managed by the Swedish Meteorological and Hydrological Institute (SMHI); and the lake monitoring stations Tärnan SSO, Megrundet N, and Dagskärsgrund N (in yellow) from the Swedish freshwater monitoring program. (For interpretation of the references to color in this figure legend, the reader is referred to the web version of this article.)

$$R_{RS}^{PRS}(\lambda) = L_{WN}^{PRS}(\lambda)/F_0(\lambda) \quad (1)$$

with the acronym *PRS* referring to the name of the in situ instrument, the Sea-Viewing Wide Field-of-View Sensor Photometer Revision for Incident Surface Measurements (SeaPRISM), and indicating AERONET-OC data. $F_0(\lambda)$ indicates the mean spectral extra-atmospheric irradiance from Thuillier et al. (2003). It is acknowledged that the uncertainties introduced by the application of corrections for bidirectional effects proposed for optical Case-1 waters (Morel et al., 2002) are unknown for the optically-complex waters of Lake Vänern. Still, their application is a best attempt to normalize the in situ data products with respect to the viewing and illumination geometries, and it is consistent with the corrections applied during the generation of the satellite radiometric data products used in this study.

Since 1973, between April and October, monthly measurements of chlorophyll-*a* concentration (*Chl-a*), filtered water absorbance at 420 nm *Abs*(420) and phytoplankton biovolume, and additionally of *turbidity* (only since 2010), have been performed within the Swedish National Freshwater Monitoring Program in Lake Vänern at the three monitoring stations shown in Fig. 1. These measurements were obtained from the Swedish University of Agricultural Sciences (SLU) environmental database in addition to measurements of total organic carbon (TOC), total nitrogen (Tot-N) and total phosphorus (Tot-P). With specific reference to these in situ data, it was noted that some laboratory methods changed over time. Because of this, the time-series used in this study were restricted to those periods characterized by the application of consistent measurement methods, and restricted to data spanning over a certain number of years.

Abs(420) values were available at the 0.5 m depth and also at various deeper depths varying with time. The samples closest to the surface were used to determine the absorption coefficient of colored dissolved organic matter at 420 nm $a_{CDOM}(420)$ according to Hu et al. (2002):

$$a_{CDOM}(420) = log10 * Abs(420)/l \quad (2)$$

where l is the path length in meters (0.05 m, for the data considered here).

In addition to the SLU data, time-series of daily precipitation P and air temperature T_A were obtained from the Swedish Meteorological and Hydrological Institute (SMHI) for stations operated along the lake shoreline (see cyan circles in Fig. 1). Finally, North Atlantic Oscillation index data were obtained from the NOAA Climate Prediction Center (NOAA, 2022).

Satellite data

To ensure temporal coherence across the investigated period, the study only relied on data from the Moderate Resolution Imaging Spectroradiometer on board the Aqua platform (MODIS-A). The relevant Level-2 data products, identified as Reprocessing R2018 (NASA, 2018), were obtained from the National Aeronautics and Space Administration (NASA). The MODIS-A mission was selected for its longer (when compared to others) and continuous time-series. It was preferred to MODIS-Terra because of its better radiometric performance at the short center-wavelengths (Meister and Franz, 2011).

Because the accuracy of MODIS-A Ocean Color radiometric products in Lake Vänern has not been assessed yet, in this work AERONET-OC data were used as a reference for MODIS-A $R_{RS}(\lambda)$ validation. For this purpose, matchups of in situ and satellite data were created applying the criteria detailed in Mélin et al. (2011). Specifically, the relevant satellite data were created using MODIS-A 3 × 3 pixels (i.e., approximately 3 × 3 km) centered at the Pålgrunden site and were retained for subsequent analysis when: i) none of the nine pixels was affected by exclusion flags; ii) the coefficient of variation (*CV*) of the nine pixels at 555 nm was lower than 20%; and iii) the time difference between in situ and satellite acquisition was 1 h at most. In order to obtain accurate spectral matching, in situ $R_{RS}(\lambda)$ at various MODIS center-wavelengths were determined from AERONET-OC data through band-shifting as described in Zibordi et al. (2009a).

For each MODIS-A band, the root mean square difference *RMSD*, the mean relative difference Ψ_m and the mean absolute (unsigned) relative difference $|\Psi|_m$ between in situ $R_{RS}^{PRS}(\lambda)$ and satellite $R_{RS}^{MODIS-A}(\lambda)$ were determined. Then, linear least-squares regressions were computed to obtain the coefficient of determination r^2.

The same criteria were applied to create matchups of in situ measurements and MODIS-A *Chl-a* (https://oceancolor.gsfc.nasa.gov/atbd/chlor_a/) and diffuse attenuation coefficient for downwelling irradiance at 490 nm $K_d(490)$ (https://oceancolor.gsfc.nasa.gov/atbd/k_d/).

In addition to MODIS-A data, satellite-derived Lake Surface Water Temperature (*LSWT*), *Chl-a* and *turbidity* from the Climate Change Initiative (CCI) product suite (Carrea et al., 2022) were also considered. After assessing their accuracy against in situ data, those products showing good performances were exploited in the following analysis. Specifically, the mean value of 3 × 3 (i.e., approximately 3 × 3 km) pixels centered at the in situ measurement stations was used, only including those pixels flagged as "best quality data".

Temporal trends and correlations

Both satellite-derived and in situ time-series were first analyzed to evaluate trends via the Seasonal Mann Kendall Test (Hirsch et al., 1982) and the seasonal Sen's Slope estimator (i.e., the median slope calculated using observation pairs from the same month across consecutive years), by applying the Python routines by Hussain and Mahmud (2019). After extracting the MODIS-A 3 × 3 pixel values corresponding to the in situ measurement stations, the Pearson correlation coefficient r_P was calculated between in situ bio-physical data and values of $R_{RS}^{MODIS-A}(\lambda)$ at a few bands, band-ratios and band-differences, selected on the basis of best results from the assessment of MODIS-A data products. Possible correlations with meteorological quantities potentially influencing the water color trends, i.e., total winter precipitation P_w (from December through March), winter mean air temperature T_{AW}, winter *NAO* (NAO_W) and *LSWT*, were also investigated.

Results

Assessment of satellite data products

As expected, due to the optical complexity and the low values of $R_{RS}(\lambda)$ in the blue spectral region, both characterizing the Lake Vänern waters, the assessment of MODIS-A radiometric products showed poor results at the shortest blue center-wavelengths (see Fig. 2). In particular, $|\Psi|_m$ exhibited values of 136% and 38% at 412 and 443 nm, respectively. Conversely, a better performance was noted beyond 443 nm with best results at the 547 and 555 nm center-wavelengths showing values of $|\Psi|_m$ around 10%. Concerning band-ratios and band-differences, the best results were observed for $R_{RS}^{MODIS-A}(547)/R_{RS}^{MODIS-A}(667)$ (hereafter indicated as $R_{547/667}$), $R_{RS}^{MODIS-A}(667)/R_{RS}^{MODIS-A}(488)$ (indicated as $R_{667/488}$), and $R_{RS}^{MODIS-A}(547) - R_{RS}^{MODIS-A}(667)$ (indicated as $D_{547\text{-}667}$) (see Fig. 3).

CCI *LSWT* assessment against in situ data showed very good performances indicated by $|\Psi|_m$ = 5% (r^2 = 0.99). Conversely, satellite and in situ *Chl-a* (from both MODIS-A and CCI products) exhibited poor agreement with r^2 < 0.1 and very large $|\Psi|_m$ values (i.e., exceeding 66% and several hundred percent for CCI and MODIS-A products, respectively). Additionally, no significant correlation was observed between MODIS-A $K_d(490)$ products and in situ *turbidity*. Finally, few matchups were obtained for CCI *turbidity* products (11 across all stations); their comparison with in situ data showed a value of $|\Psi|_m$ exceeding 35% with r^2 = 0.02. Because of these results, *Chl-a*, $K_d(490)$ and *turbidity* satellite products were not further investigated.

Trends characterizing MODIS-A and in situ time-series

Given the results summarized above, which support a confident use of MODIS-A satellite radiometric data, temporal analyses were performed relying on values at selected center-wavelengths ($R_{RS}^{MODIS-A}(\lambda)$ with λ = 488, 547 and 667 nm), and specific band-ratios and band-differences ($R_{547/667}^{MODIS-A}$, $R_{667/488}^{MODIS-A}$ and $D_{547-667}^{MODIS-A}$). It is recalled that $R_{RS}(667)$ is commonly used to investigate high *turbidity* or surface accumulation of cyanobacteria (Kahru and Elmgren, 2014) as its increase usually results from enhanced backscattering of particles. $R_{RS}(560)$ can also be considered as an index for water clarity in lakes (Binding et al., 2015). The red-blue ratio $R_{667/488}^{MODIS-A}$ was identified as potential indicator for *CDOM* concentration. In particular, considering that *CDOM* absorption is greater at shorter center-wavelengths and exponentially decreases with increasing wavelength, Kutser et al. (2009) reported that in boreal *CDOM*-rich lakes a green-to-red ratio would be more robust with respect to atmospheric correction errors, glint perturbations and low signal-to-noise ratios. Consequently, the $R_{547/667}^{MODIS-A}$ was also included. It is also mentioned that $R_{547/667}^{MODIS-A}$ was used to retrieve the diffuse attenuation coefficient in turbid coastal waters (Wang et al., 2009). Finally, despite the fact that the phytoplankton absorption maximum is located in the blue spectral region where satellite radiometric products do not show reliable values in most boreal lake waters, a second absorption peak characterizes the red

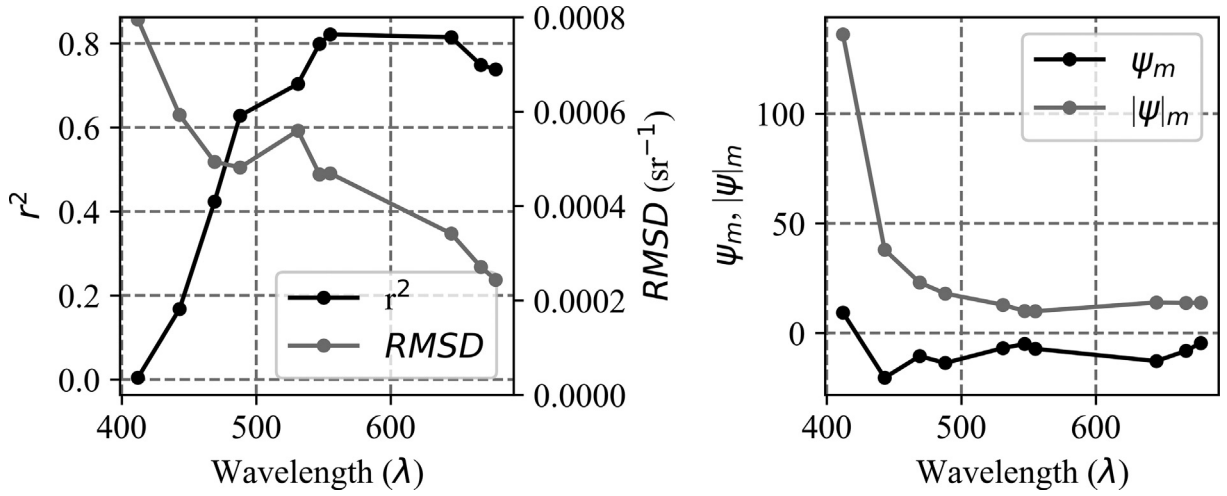

Fig. 2. Results from the comparison of MODIS-A $R_{RS}^{MODIS-A}(\lambda)$ with AERONET-OC $R_{RS}^{PRS}(\lambda)$ at Pålgrunden: (a) values of the coefficient of determination r^2 and of the root mean square difference *RMSD*; (b) the mean relative difference Ψ_m and the mean absolute (unsigned) relative differences $|\Psi|_m$, both expressed in %.

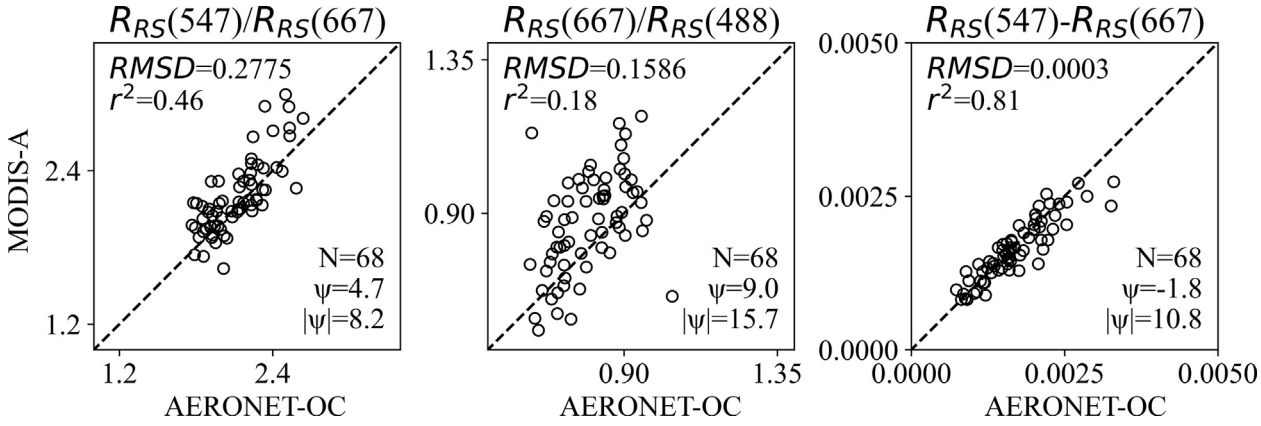

Fig. 3. Scatterplots of MODIS-A versus AERONET-OC matchup data for selected band-ratios and band-differences.

spectral region around 670 nm (see for example Fig. 7a in Reinart et al., 2004). Consequently, $D_{547-667}^{MODIS-A}$ was also included in the analysis. Additionally, band-differences are expected to be more robust than band-ratios to atmospheric correction (Hu et al., 2012; Hu, 2009; Mitchell et al., 2017) as confirmed by the results presented above.

The results from the analysis of $R_{RS}^{MODIS-A}(\lambda)$ are summarized in Fig. 4 and show periodic changes between 2002 and 2021 with clear minima occurring between 2010 and 2013. Spring maxima take place during 2005–2008 and in 2020, followed by a decrease in 2021. A large increase of $R_{RS}^{MODIS-A}(\lambda)$ is notable from 2015 until 2020 at Megrundet N. Conversely, the band-ratios exhibit different trends varying with season. $R_{547/667}^{MODIS-A}$ shows spring maxima during 2008 and 2009, followed by relatively low values between 2012 and 2020. $R_{667/488}^{MODIS-A}$ indicates maxima in 2002 and 2003, and again from 2012 to 2015, and a successive decrease in 2020.

The highest concentration of in situ *Chl-a* data was recorded at Dagskärsgrund N at the beginning of the time-series (see Fig. 5, panel a) with values higher than 6 μg L^{-1}. Despite that, from 1973 to 2021 in situ *Chl-a* exhibits positive trends at all stations as shown by the Sen's Slope values reported in Table 1. Conversely, $a_{CDOM}(420)$ data are characterized by decreasing values since the 1970s, even though they exhibit periodic variations with relative maxima occurring at the beginning of the 2000s and between 2012 and 2015 (see Fig. 5, panel b). The values of $a_{CDOM}(420)$ are relatively low at Megrundet N compared to the other measurement locations. On the contrary, *turbidity* exhibits relatively higher values and a positive trend during recent years (see Table 1). The total phytoplankton biovolume (hereafter total biovolume) shows large periodical changes with clear maxima occurring during spring in 2002, 2005 and 2020 (Fig. 5d). At Megrundet N and Tärnan SSO lower values of total biomass were typically recorded in April after winter seasons characterized by the presence of ice-cover such as in 1996, 2003, 2006, 2010, 2018 (data from SMHI), confirming earlier findings by Weyhenmeyer et al. (2008).

Note that before 1996, no in situ data were collected in the month of April, which is usually characterized by a phytoplankton spring bloom in the western basin.

In view of the comprehensive benefit of the synoptic view enabled by satellite data products, yearly spring mean values of $R_{RS}^{MODIS-A}(667)$ are displayed in Fig. 6. Corresponding time-series of $R_{RS}^{MODIS-A}(667)$ are displayed in Fig. 7 for Tärnan SSO, Megrundet N and Pålgrunden measurement sites. Noting that $R_{RS}^{MODIS-A}(667)$ is a natural index for water *turbidity*, both figures show marked temporal changes and often clear differences between the two basins with an increase in $R_{RS}(\lambda)$ from 2015 similar to that observed in AERONET-OC data at Pålgrunden, but more pronounced in MODIS-A data at Megrundet N. Consistently, the maps in Fig. 6 show the highest mean values in 2015 and 2020 in the western

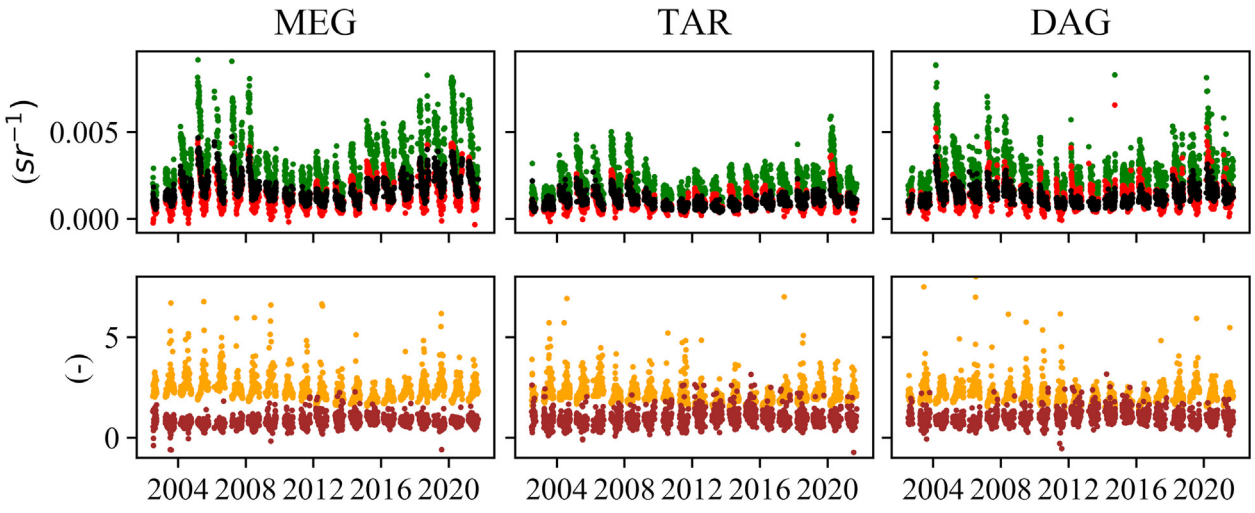

Fig. 4. Time-series of $R_{RS}^{MODIS-A}(\lambda)$ at 547 nm (green dots) and 667 nm (red dots) center-wavelengths and $D_{547-667}^{MODIS-A}$ (black dots) displayed in the first row, and additionally, of $R_{547/667}^{MODIS-A}$ (orange dots) and $R_{667/488}^{MODIS-A}$ (brown dots) displayed in the second row. Data refer to the Megrundet N (MEG, first column from the left), Tärnan SSO (TAR, second column) and Dagskärsgrund N (DAG, third column) sites. Some $R_{547/667}^{MODIS-A}$ outliers are not displayed as to improve visualization. (For interpretation of the references to color in this figure legend, the reader is referred to the web version of this article.)

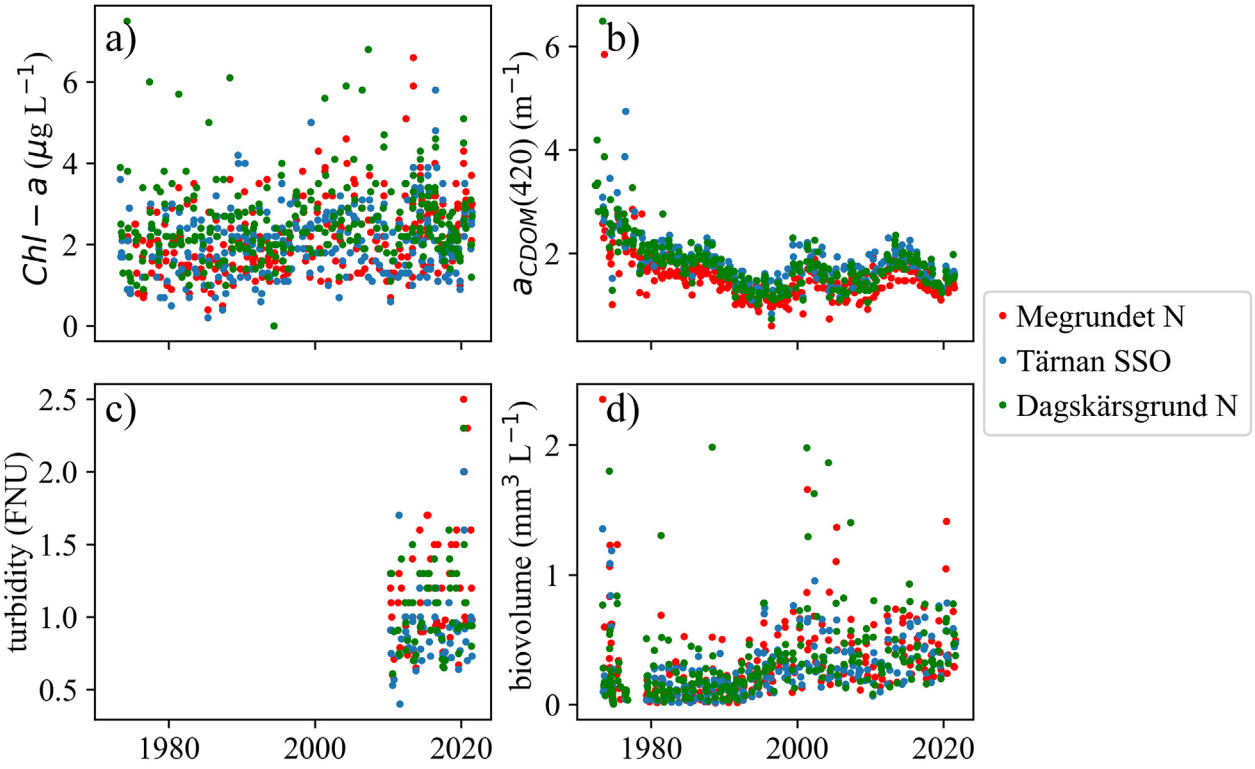

Fig. 5. Time-series of (a) *Chl-a*, (b) $a_{CDOM}(420)$, (c) *turbidity* and (d) biovolume at the three lake monitoring stations shown in Fig. 1.

Table 1
Results from the Sen's Slope trend analysis for in situ *Chl-a*, $a_{CDOM}(420)$, *turbidity* and total biovolume measurements from the three in situ measurement stations. Note that negative values indicate decreasing trends.

	Chl-a ($\mu g\ L^{-1}\ y^{-1}$)	$a_{CDOM}(420)$ ($m^{-1}\ y^{-1}$)	biovolume ($mm^3\ L^{-1}\ y^{-1}$)	*turbidity* (FNU y^{-1})
Tärnan SSO	0.015	−0.015	0.008	no trend
Megrundet N	0.017	−0.012	0.005	0.05
Dagskärsgrund N	0.007	−0.017	0.004	no trend

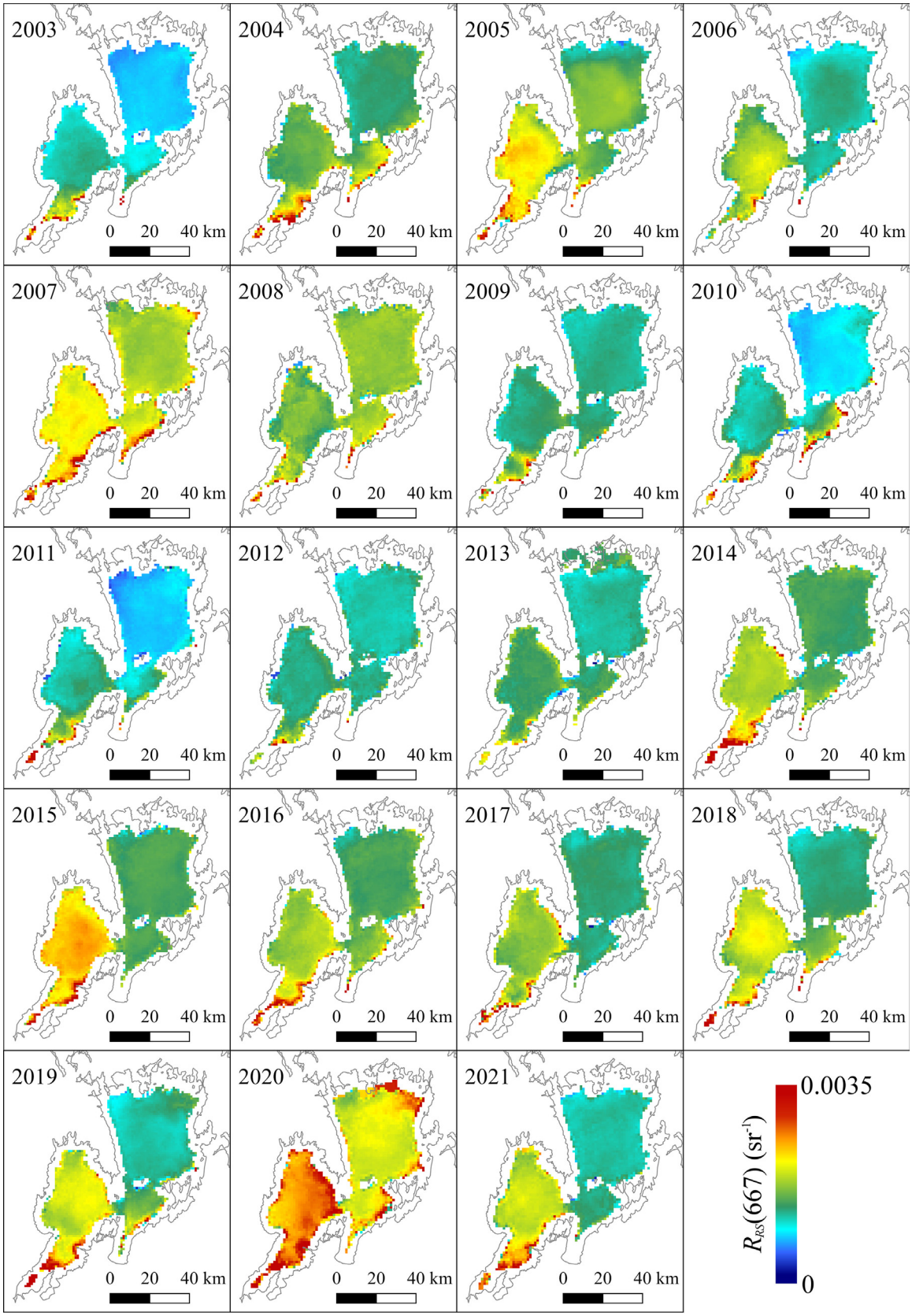

Fig. 6. Maps of mean $R_{RS}^{MODIS-A}(667)$ determined for the spring season from 2003 until 2021. The lake shoreline is indicated in grey and has been obtained from Lehner and Döll (2004).

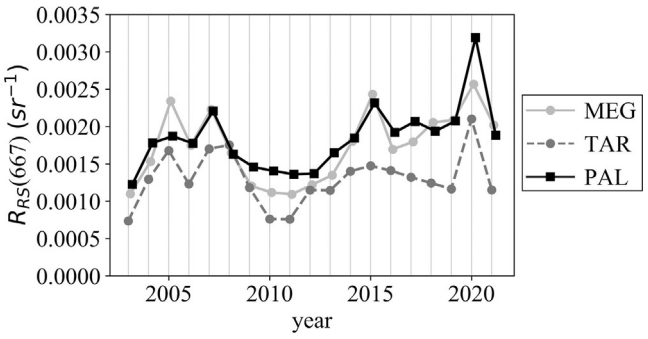

Fig. 7. $R_{RS}^{MODIS-A}(667)$ spring mean obtained from the data at Megrundet N (MEG), Tärnan SSO (TAR) and Pålgrunden (PAL) locations shown in Fig. 6.

basin when *turbidity* also shows its maxima (see Fig. 5c). Conversely, relatively smaller temporal changes appear to characterize the eastern basin, although exhibiting peak values in 2007 and 2020. Fig. 7 shows that the values of $R_{RS}^{MODIS-A}(667)$ at Pålgrunden follow a similar trend as shown for Megrundet N (western basin), whereas the reflectance is substantially lower at Tärnan SSO, where relative maxima are observed in 2015 and 2020. These trends show patterns similar to those observed for the in situ *turbidity* data in spring (see Fig. 5c).

Correlations between $R_{RS}(\lambda)$ and bio-physical quantities

The correlation coefficients r_p have been determined between in situ bio-physical data and $R_{RS}^{MODIS-A}(\lambda)$ at 488, 547 and 667 nm, or, alternatively, $R_{RS}^{MODIS-A}(\lambda)$ band-ratios or band-differences. The most pronounced correlations are observed at Megrundet N and Tärnan SSO between in situ *turbidity* and $R_{RS}^{MODIS-A}(\lambda)$ or alternatively $D_{547-667}^{MODIS-A}$. At the same locations, in situ *turbidity* shows a negative correlation with $R_{547/667}^{MODIS-A}$.

A good correlation has also been determined at Megrundet N between the total biovolume and $R_{RS}^{MODIS-A}(\lambda)$, or alternatively $D_{547-667}^{MODIS-A}$, with higher values characterizing the months of April and May (e.g., r_p = 0.7 $R_{RS}^{MODIS-A}(547)$). Conversely, $a_{CDOM}(420)$ at Dagskärsgrund N showed a positive correlation with $R_{667/488}^{MODIS-A}$ and a negative correlation with $R_{RS}^{MODIS-A}(488)$, $R_{547/667}^{MODIS-A}$ or $D_{547-667}^{MODIS-A}$. However, $a_{CDOM}(420)$ at Tärnan SSO showed a low correlation with both $R_{667/488}^{MODIS-A}$ and $R_{547/667}^{MODIS-A}$. Finally, a weak correlation has been determined at Dagskärsgrund N between $R_{RS}^{MODIS-A}(667)$ and *Chl-a* (r_p = 0.37). The significant correlations exhibiting *p-value* < 0.05 are illustrated in Fig. 8.

Correlations between $R_{RS}(\lambda)$ and meteo-climatic quantities

Based on the analysis of in situ time-series of air temperature and total biomass between 1979 and 1999 for several stations in Lake Vänern, Weyhenmeyer (2001) noted that the spring phytoplankton bloom declines earlier with warmer winters, which suggests an earlier growth season. For this reason, any possible correlation between spring biovolumes and T_{AW}, P_W and NAO_W was investigated. However, a positive correlation with the April biovolume was only observed at Megrundet N for T_{AW} and NAO_W (i.e., with r_p = 0.48 and 0.45, respectively). Conversely, appreciable correlations are not observed for the diatom share of the biovolume.

The value of r_p was determined for mean spring (i.e., from March to May) $R_{RS}^{MODIS-A}(\lambda)$ or band-ratios, with respect to P_W, T_{AW} and NAO_W meteo-climatic quantities. The highest correlation values, with r_p varying between 0.59 and 0.73, were observed at Tärnan SSO between $R_{RS}^{MODIS-A}(\lambda)$ and T_{AW}. At Dagskärsgrund N, $R_{RS}^{MODIS-A}(\lambda)$ was only well correlated with P_W (r_p between 0.62 and 0.75). Finally, at Megrundet N only, some weak correlation was observed with T_{AW} and P_W with r_p varying between 0.45 and 0.59. NAO_W is only correlated with $R_{RS}^{MODIS-A}(667)$ at Megrundet N and Tärnan SSO with r_p = 0.48 and 0.56, respectively.

Discussion

Results from the trend analysis showed a temporal variability for various parameters (e.g., $a_{CDOM}(420)$, $R_{RS}(\lambda)$). What causes these fluctuations and the notable increase in $R_{RS}(\lambda)$ in the western basin since 2015?

Results show that a good correlation is observed for both $R_{RS}^{MODIS-A}(\lambda)$ (at 488, 547 and 667 nm) and $D_{547-667}^{MODIS-A}$ with the total biovolume at Megrundet N (see Fig. 8), whereas no correlation is found at Tärnan SSO. The biovolume, indeed, exhibits diverse temporal dependences for the two sites with seasonal differences more pronounced at Megrundet N with respect to Tärnan SSO. Since the beginning of the time-series in 1973, diatoms clearly dominate the total biovolume in spring with a gradual increase, more marked at Megrundet N. Since 2006, the *cyanobacteria* and *cryptophyta* biovolumes show an increase in May. In April, the total biovolume is generally higher at Megrundet N, when $R_{RS}^{MODIS-A}(\lambda)$ exhibits its maxima (see Fig. 9). At Tärnan SSO, however, the total biovolume usually shows maxima in May – June. It must be noted that in situ measurements for the month of July are very sparse and only available for 2002 and 2019.

The time-series of monitoring data at Megrundet N and Tärnan SSO further confirm the difference between the two basins. Fig. 10 displays the time-series of TOC and nutrients represented here as Tot-N, and Tot-P. The latter shows a time-series perturbed by periodic changes and a weak correlation with $a_{CDOM}(420)$ with r_p equal to 0.42 and 0.36 at Tärnan SSO and Megrundet N, respectively. TOC, exhibiting minima in 2019, is generally lower at Megrundet N than at Tärnan SSO. Also, Tot-N is generally higher at Tärnan SSO than at Megrundet N: it decreases until 2019, with a new increase at both sites in 2020. Conversely, mean Tot-P is slightly higher at Megrundet N, although its variability is higher at Tärnan SSO where it shows maxima.

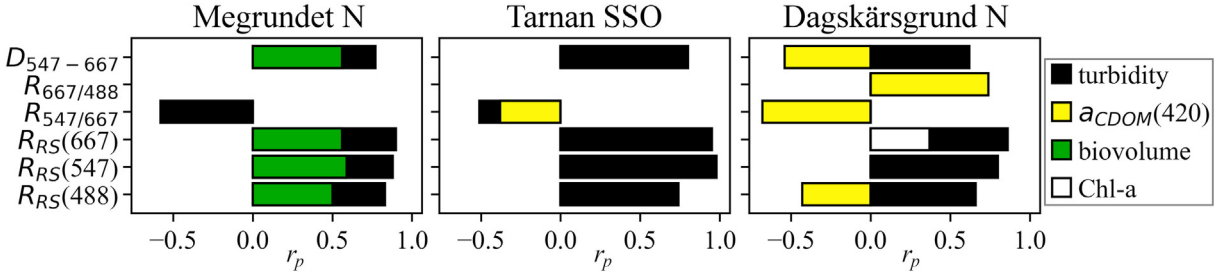

Fig. 8. Correlations r_p between $R_{RS}^{MODIS-A}(\lambda)$ at selected bands, band-ratios, and band-differences with in situ bio-physical data values.

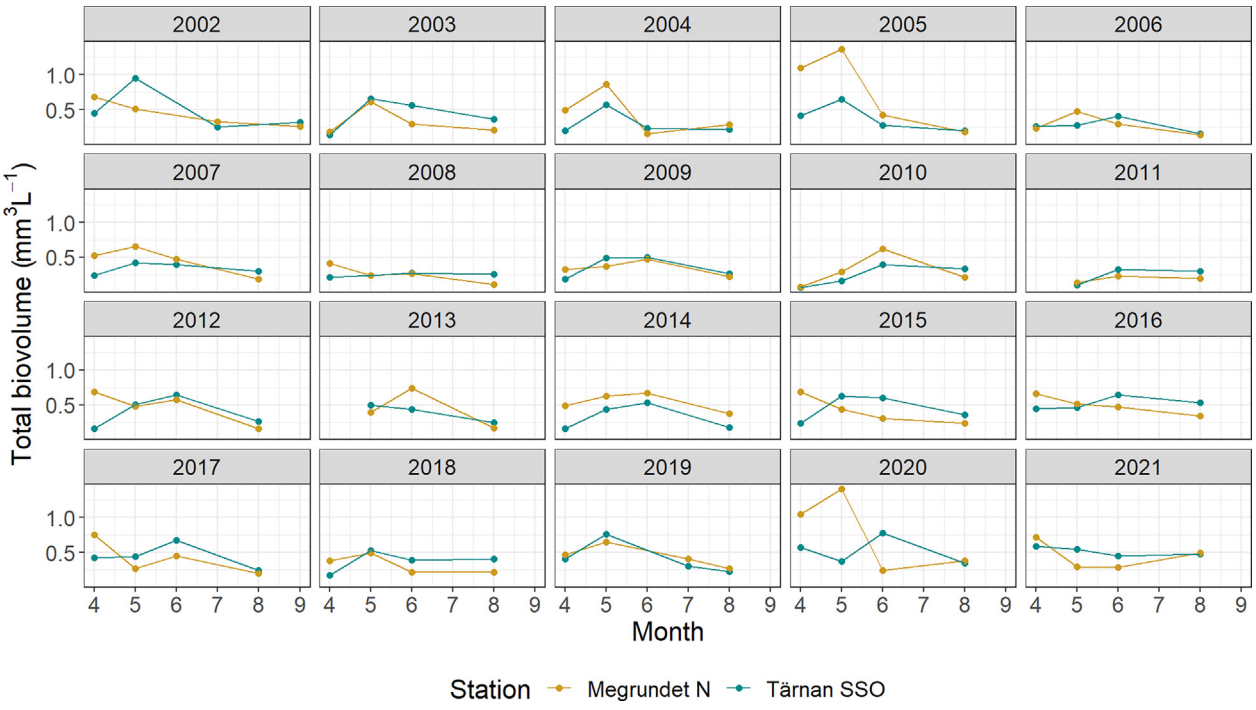

Fig. 9. Total biovolume measured at the Megrundet N and Tärnan SSO stations.

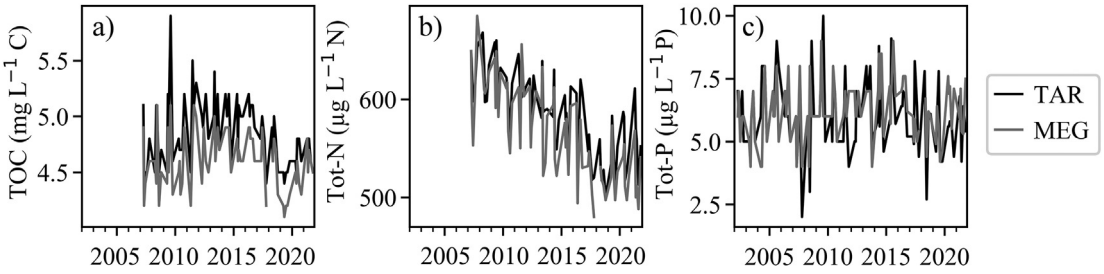

Fig. 10. In situ measurements at Megrundet N (MEG, in grey) and Tärnan SSO (TAR, in black) for a) total organic carbon (TOC), b) total organic nitrogen (Tot-N) and c) total phosphorus (Tot-P). For each parameter, data are only shown for the most recent period characterized by the application of the same measurement methods.

Overall, the analyses suggest complex and concurrent biogeochemical processes influencing the spectral reflectance of Lake Vänern. In an attempt to further identify the causes for the observed temporal changes in $R_{RS}(\lambda)$ at Lake Vänern, the occurrence of the thermal bar effect has been investigated. This physical process usually occurs in spring and prevents the shallow (with depth < 20 m, Håkanson, 1977), generally more turbid waters of the southern part of the western basin from mixing with those in the central lake region. To explore this process, in situ water temperature and satellite *LSWT* data were analyzed at the monitoring stations, and additionally in the shallower southern region. In particular, the day of the year (*doy*) when *LSWT* reaches 4 °C during the spring season (indicated as doy_{4C}) was determined. Considering that the satellite *LSWT* against in situ data showed a very high correlation supported by $|\Psi|_m$ = 5% (r^2 = 0.99), in situ and satellite derived *LSWT* time-series were subsequently merged for further analysis. Recognizing that an irregular temporal distribution of data may strongly influence the results, the data beyond 2005 were the sole considered to ensure a higher statistical representativity of the time-series. At the southern point ('SOUTH' in Fig. 11), the doy_{4C} minimum is observed in 2014 and in 2020. The difference between doy_{4C} in the southern region and Megrundet N may vary from a few days (in 2010, 2013 and 2020), up to three weeks (in 2012). Doy_{4C} is usually higher at Tärnan SSO than at Megrundet N, whereas the Dagskärsgrund N doy_{4C} is similar to that characterizing the southern region.

Since 2014 doy_{4C} has usually occurred earlier at all the locations. This is both shown in the time-series (Fig. 11a) and in the Hovmöller diagram (Fig. 11b). Between 2005 and 2013 doy_{4C} was close to *doy* 127 at Megrundet N (average value); whereas, between 2014 and 2020, it was on average 117 with 2020 showing the lowest doy_{4C} (i.e., 107). Additionally, from 2014 *LSWT* increased much faster in spring than in the previous decade, except for 2018 when the lake was covered by ice.

The years during which the water temperature reached 4 °C later in the season (e.g., 2009–2013) showed lower $R_{RS}^{MODIS-A}(\lambda)$ values (Fig. 4 upper panel). Several studies reported shifts in phytoplankton phenology associated with changes in the thermal stratification of lakes (e.g., Domis De Senerpont et al., 2013; Winder and Schindler, 2004). In particular, Winder and Schindler (2004) documented that the increase in the thermal stratification period was mainly caused by an earlier spring stratification. Phytoplankton phenological shifts were also linked to both local processes and climate change by Thackeray et al. (2008). Maeda

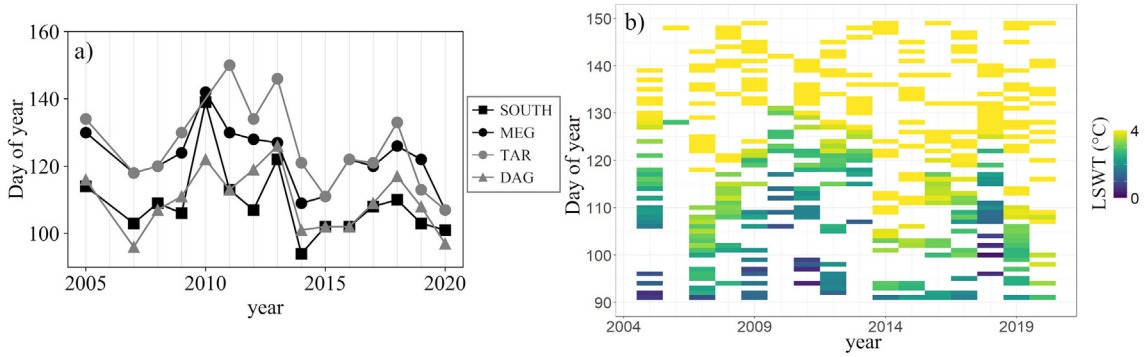

Fig. 11. a) First day of the year when *LSWT* exceeded 4 °C (doy_{4C}) at the three in situ measurement stations (Megrundet N, Tärnan SSO and Dagskärsgrund N) and the additional southern location (SOUTH). b) *LSWT* spring evolution at Megrundet N shown as Hovmöller diagram.

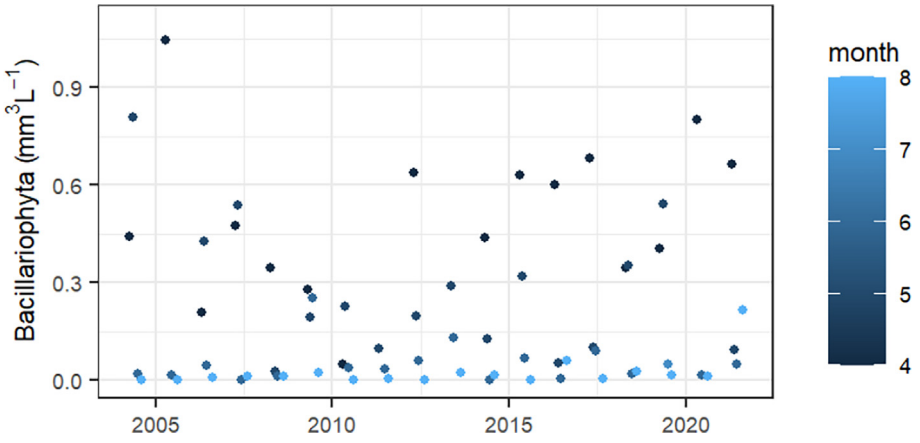

Fig. 12. Changes in diatom biomass during the study period at Megrundet N station. Colors vary depending on the month of the measurement.

et al. (2019) instead showed that the earlier spring onset could be influenced by changes in precipitation patterns in high latitude lakes in Finland. In fact, they did not find any correlation between lake surface temperature and phenological trends. However, they could not exclude the influence of any process linked to temporal changes in the thermal stratification of these lakes.

The years during which the water temperature increased earlier in Lake Vänern (e.g., 2005–2008 and 2014–2020, 2018 excluded) exhibit increased *turbidity* and a higher diatom biomass in spring (see Fig. 12), which is also mirrored by higher $R_{RS}^{MODIS-A}(\lambda)$. This suggests that the temporal increase in the in situ $R_{RS}(\lambda)$ measured in Lake Vänern tends to be explained by the combined effect of meteo-climatic and biological variables.

Conclusion

AERONET-OC data from the Pålgrunden site in Lake Vänern clearly showed increasing values of $R_{RS}(\lambda)$ across the whole spectrum since 2015: this suggests changes in water color due to bio-geochemical and physical processes. AERONET-OC data, however, were only collected since 2008. To overcome such a limitation in the temporal availability of data, MODIS-A $R_{RS}(\lambda)$ time-series were analyzed to allow for investigating radiometric data products from 2002 and to additionally cover periods of the year when the Pålgrunden AERONET-OC instrument was not operated. Still, confidence in MODIS-A $R_{RS}(\lambda)$ data is provided by their assessment against AERONET-OC data showing best agreement in the green spectral bands and for some specific $R_{RS}(\lambda)$ band-ratios and band-differences (i.e., $R_{547/667}^{MODIS-A}$, $R_{667/488}^{MODIS-A}$ and $D_{547-667}^{MODIS-A}$).

Consequently, the MODIS-A time-series allowed to explore the temporal changes characterizing $R_{RS}(\lambda)$ data not detectable when solely considering the shorter AERONET-OC time-series data restricted to the Pålgrunden location. In particular, while the MODIS-A $R_{RS}(\lambda)$ time-series shows high values between 2004 and 2008, and successively between 2015 and 2020 at Pålgrunden, the data analyses extended to diverse locations with the additional contribution of in situ bio-geochemical measurements, exhibit a more marked increase in $R_{RS}(\lambda)$ since 2015 in the western basin of Lake Vänern with respect to the eastern one. The values of bio-geochemical parameters at specific measurement locations further confirm differences between the two basins: however, they do not allow unequivocally to ascertain the cause for the increase in $R_{RS}(\lambda)$. Still, some correlations between bio-geochemical variables and $R_{RS}(\lambda)$ have been identified. In particular, significant correlations have been observed between $R_{RS}(\lambda)$ and *turbidity* values in both basins at the Megrundet N and Tärnan SSO measurement sites. Correlations with total biovolume have only been observed in the western basin at the Megrundet N site. At Dagskärsgrund N, in the eastern basin, significant correlations have also been observed with $a_{CDOM}(420)$ and *Chl-a*.

Additional elements supporting the complexity of the bio-geochemical and physical processes characterizing temporal changes at Lake Vänern are the observed correlations between the phytoplankton biovolume measured in April (when the major algal blooms usually occur) with winter mean air temperature T_{AW} and winter North Atlantic Oscillation index NAO_W. Finally, a further relevant finding is an earlier seasonal warming of Lake Vänern surface waters since 2014 leading to an earlier thermal bar break-up with respect to the previous decade. In addition to

the impact on diatom biomass and in general on phytoplankton phenology, this also potentially affects the water exchange between the more turbid southern coastal waters and the pelagic waters in the western basin.

CRediT authorship contribution statement

Ilaria Cazzaniga: Formal analysis, Software, Investigation, Validation, Visualization, Methodology, Writing – original draft, Writing – review & editing. **Giuseppe Zibordi:** Formal analysis, Investigation, Supervision, Funding acquisition, Writing – review & editing. **Krista Alikas:** Formal analysis, Visualization, Investigation, Writing – review & editing. **Susanne Kratzer:** Funding acquisition, Writing – review & editing.

Declaration of Competing Interest

The authors declare that they have no known competing financial interests or personal relationships that could have appeared to influence the work reported in this paper.

Acknowledgments

The authors would like to thank the AERONET team for processing and distributing the data from the Ocean Color component of the Aerosol Robotic Network, and NASA OB.DAAC for granting access to the MODIS-A data. The Swedish Agency for Marine and Water Management and the NOAA/National Weather Service are also acknowledged for the meteo-climatic data. The in situ data from SLU's environmental database for soil-water-environment have been funded by the Swedish Environmental Protection Agency within the framework of a national coordinated environmental monitoring program. The Swedish National Space Agency is acknowledged for the long-term funding of the AERONET-OC Pålgrunden site (SNSA Grant 2021-00050). Finally, extreme gratitude is expressed to the Pålgrunden site manager Niklas Strömbeck for his support to AERONET-OC field operations since the first instrument deployment in 2008.

References

Anderson, N.J., 2000. Miniview: Diatoms, temperature and climatic change. Eur. J. Phycol. 35, 307–314. https://doi.org/10.1080/09670260010001735911.

Binding, C.E., Greenberg, T.A., Watson, S.B., Rastin, S., Gould, J., 2015. Long term water clarity changes in North America's Great Lakes from multi-sensor satellite observations. Limnol. Oceanogr. 60, 1976–1995. https://doi.org/10.1002/lno.10146.

Carrea, L., Crétaux, J.-F., Liu, X., Wu, Y., Bergé-Nguyen, M., Calmettes, B., Duguay, C., Jiang, D., Merchant, C.J., Mueller, D., Selmes, N., Simis, S., Spyrakos, E., Stelzer, K., Warren, M., Yesou, H., Zhang, D., 2022. ESA Lakes Climate Change Initiative (Lakes_cci): Lake Products, Version 2.0.2. NERC EDS Centre for Environmental Data Analysis. 06 July 2022. doi:10.5285/a07deacaffb8453e93d57ee214676304.

Dahl, M., Pers, B.C., 2004. Comparison of four models simulating phosphorus dynamics in Lake Vänern, Sweden. Hydrol. Earth Syst. Sci. 8, 1153–1163. https://doi.org/10.5194/hess-8-1153-2004.

de Wit, H.A., Valinia, S., Weyhenmeyer, G.A., Futter, M.N., Kortelainen, P., Austnes, K., Hessen, D.O., Räike, A., Laudon, H., Vuorenmaa, J., 2016. Current browning of surface waters will be further promoted by wetter climate. Environ. Sci. Technol. Lett. 3, 430–435. https://doi.org/10.1021/acs.estlett.6b00396.

Domis De Senerpont, N.L., Elser, J.J., Gsell, A.S., Huszar, V.L.M., Ibelings, B.A.S.W., Jeppesen, E., Kosten, S., Mooij, W.M., Roland, F., Sommer, U., Van Donk, E., Winder, M., Lürling, M., 2013. Plankton dynamics under different climatic conditions in space and time. Freshw. Biol. 58, 463–482. https://doi.org/10.1111/fwb.12053.

ESA, 2021. Lakes CCI project Key Documents. D4.3: Product User Guide (PUG) - CCI-LAKES-0029-PUG.

ESPON, 2021. REGIONAL REPORT. Lake Vänern Inner periphery seeking a new start. Annex to synthesis report.

Håkanson, L., 1977. The influence of wind, fetch, and water depth on the distribution of sediments in Lake Vänern, Sweden. Can. J. Earth Sci. 14 (3), 397–412.

Hirsch, R.M., Slack, J.R., Smith, R.A., 1982. Techniques of trend analysis for monthly water quality data. Water Resour. Res. 18, 107–121. https://doi.org/10.1029/WR018i001p00107.

Hrycik, A.R., Isles, P.D.F., Adrian, R., Albright, M., Bacon, L.C., Berger, S.A., Bhattacharya, R., Grossart, H.P., Hejzlar, J., Hetherington, A.L., Knoll, L.B., Laas, A., McDonald, C.P., Merrell, K., Nejstgaard, J.C., Nelson, K., Nõges, P., Paterson, A. M., Pilla, R.M., Robertson, D.M., Rudstam, L.G., Rusak, J.A., Sadro, S., Silow, E.A., Stockwell, J.D., Yao, H., Yokota, K., Pierson, D.C., 2021. Earlier winter/spring runoff and snowmelt during warmer winters lead to lower summer chlorophyll-a in north temperate lakes. Glob. Chang. Biol. 27, 4615–4629. https://doi.org/10.1111/gcb.15797.

Hu, C., 2009. A novel ocean color index to detect floating algae in the global oceans. Remote Sens. Environ. 113, 2118–2129. https://doi.org/10.1016/j.rse.2009.05.012.

Hu, C., Muller-Karger, F.E., Zepp, R.G., 2002. Absorbance, absorption coefficient, and apparent quantum yield: A comment on common ambiguity in the use of these optical concepts. Limnol. Oceanogr. 47, 1261–1267. https://doi.org/10.4319/lo.2002.47.4.1261.

Hu, C., Lee, Z., Franz, B., 2012. Chlorophyll *a* algorithms for oligotrophic oceans: A novel approach based on three-band reflectance difference. J. Geophys. Res. Ocean. 117 (C1).

Hussain, M.M., Mahmud, I., 2019. pyMannKendall: a python package for non parametric Mann Kendall family of trend tests. J. Open Source Softw. 4, 1556. https://doi.org/10.21105/joss.01556.

Johansson, L., Temnerud, J., Abrahamsson, J., Kleja, D.B., 2010. Variation in organic matter and water color in Lake Mälaren during the past 70 years. Ambio 39, 116–125. https://doi.org/10.1007/s13280-010-0019-2.

Kahru, M., Elmgren, R., 2014. Multidecadal time series of satellite-detected accumulations of cyanobacteria in the Baltic Sea. Biogeosciences 11, 3619–3633. https://doi.org/10.5194/bg-11-3619-2014.

Klante, C., Larson, M., Persson, K.M., 2021. Brownification in Lake Bolmen, Sweden, and its relationship to natural and human-induced changes. J. Hydrol. Reg. Stud. 36,. https://doi.org/10.1016/j.ejrh.2021.100863 100863.

Kritzberg, E.S., 2017. Centennial-long trends of lake browning show major effect of afforestation. Limnol. Oceanogr. Lett. 2, 105–112. https://doi.org/10.1002/lol2.10041.

Kritzberg, E.S., Hasselquist, E.M., Škerlep, M., Löfgren, S., Olsson, O., Stadmark, J., Valinia, S., Hansson, L.-A., Laudon, H., 2020. Browning of freshwaters: Consequences to ecosystem services, underlying drivers, and potential mitigation measures. Ambio 49 (2), 375–390. https://doi.org/10.1007/s13280-019-01227-5.

Kutser, T., Tranvik, L., Pierson, D.C., 2009. Variations in colored dissolved organic matter between boreal lakes studied by satellite remote sensing. J. Appl. Remote Sens. 3,. https://doi.org/10.1117/1.3184437 033538.

Kvarnäs, H., 2001. Morphometry and hydrology of the four large Lakes of Sweden. AMBIO A J. Hum. Environ. 30, 467. https://doi.org/10.1639/0044-7447(2001)030[0467:mahotf]2.0.co;2.

Larson, M., 2012. Sweden's Great Lakes. In: Bengtsson, L., Herschy, R.W., Fairbridge, R.W. (Eds.), Encyclopedia of Lakes and Reservoirs. Springer, Netherlands, Dordrecht, pp. 761–764. https://doi.org/10.1007/978-1-4020-4410-6_269.

Lehner, B., Döll, P., 2004. Development and validation of a global database of lakes, reservoirs and wetlands. J. Hydrol. 296 (1–4), 1–22.

Maeda, E.E., Lisboa, F., Kaikkonen, L., Kallio, K., Koponen, S., Brotas, V., Kuikka, S., 2019. Temporal patterns of phytoplankton phenology across high latitude lakes unveiled by long-term time series of satellite data. Remote Sens. Environ. 221, 609–620. https://doi.org/10.1016/j.rse.2018.12.006.

Meister, G., Franz, B.A., 2011. Adjustments to the MODIS Terra radiometric calibration and polarization sensitivity in the 2010 reprocessing. Earth Obs. Syst. XVI 8153,. https://doi.org/10.1117/12.891787 815308.

Mélin, F., Zibordi, G., Berthon, J.-F., Bailey, S., Franz, B., Voss, K., Flora, S., Grant, M., 2011. Assessment of MERIS reflectance data as processed with SeaDAS over the European seas. Opt. Express 19, 25657. https://doi.org/10.1364/OE.19.025657.

Mitchell, C., Hu, C., Bowler, B., Drapeau, D., Balch, W.M., 2017. Estimating particulate inorganic carbon concentrations of the global ocean from ocean color measurements using a reflectance difference approach. J. Geophys. Res. Ocean. 122, 8707–8720. https://doi.org/10.1002/2017JC013146.

Morel, A., Antoine, D., Gentili, B., 2002. Bidirectional reflectance of oceanic waters: accounting for Raman emission and varying particle scattering phase function. Appl. Opt. 41, 6289–6306. https://doi.org/10.1364/AO.41.006289.

NASA Goddard Space Flight Center, Ocean Ecology Laboratory, Ocean Biology Processing Group, 2018. Moderate-resolution Imaging Spectroradiometer (MODIS) Aqua Ocean Color Data; 2018 Reprocessing. NASA OB.DAAC, Greenbelt, MD, USA. doi: data/10.5067/AQUA/MODIS/L2/OC/2018. Last accessed on 12/10/2021.

NOAA, 2022. National Weather Service. NOAA Climate Prediction Center. URL address: https://www.cpc.ncep.noaa.gov/products/precip/CWlink/pna/nao.shtml, last accessed on 11 April 2022.

Philipson, P., Kratzer, S., Ben Mustapha, S., Strömbeck, N., Stelzer, K., 2016. Satellite-based water quality monitoring in Lake Vänern, Sweden. Int. J. Remote Sens. 37 (16), 3938–3960. https://doi.org/10.1080/01431161.2016.1204480.

Reinart, A., Paavel, B., Pierson, D., Strombeck, N., 2004. Inherent and apparent optical properties of Lake Peipsi, Estonia. Boreal Environ. Res. 9 (5), 429–445.

Sandström, A., Ragnarsson-Stabo, H., Axenrot, T., Bergstrand, E., 2014. Has climate variability driven the trends and dynamics in recruitment of pelagic fish species in Swedish Lakes Vänern and Vättern in recent decades? Aquat. Ecosyst. Heal. Manag. 17 (4), 349–356.

Thackeray, S.J., Jones, I.D., Maberly, S.C., 2008. Long-term change in the phenology of spring phytoplankton: species-specific responses to nutrient enrichment and climatic change. J. Ecol. 96, 523–535.

Thuillier, G., Hersé, M., Labs, D., Foujols, T., Peetermans, W., Gillotay, D., Simon, P.C., Mandel, H., 2003. The solar spectral irradiance from 200 to 2400 nm as measured by the SOLSPEC spectrometer from the Atlas and Eureca Missions. Sol. Phys. 214, 1–22. https://doi.org/10.1023/A:1024048429145.

Tyler, A.N., Hunter, P.D., Spyrakos, E., Groom, S., Constantinescu, A.M., Kitchen, J., 2016. Developments in Earth observation for the assessment and monitoring of inland, transitional, coastal and shelf-sea waters. Sci. Total Environ. 572, 1307–1321. https://doi.org/10.1016/j.scitotenv.2016.01.020.

Wang, M., Son, S., Harding, L.W., 2009. Retrieval of diffuse attenuation coefficient in the Chesapeake Bay and turbid ocean regions for satellite ocean color applications. J. Geophys. Res. 114, C10011. https://doi.org/10.1029/2009JC005286.

Weyhenmeyer, G.A., 2001. Warmer winters: Are planktonic algal populations in Sweden's largest lakes affected? Ambio 30, 565–571.

Weyhenmeyer, G.A., Westöö, A.-K., Willén, E., 2008. Increasingly ice-free winters and their effects on water quality in Sweden's largest lakes. In: Nõges, T., Eckmann, R., Kangur, K., Nõges, P., Reinart, A., Roll, G., Simola, H., Viljanen, M. (Eds.), European Large Lakes Ecosystem Changes and Their Ecological and Socioeconomic Impacts. Springer Netherlands, Dordrecht, pp. 111–118.

Weyhenmeyer, G.A., Prairie, Y.T., Tranvik, L.J., Iwata, T., 2014. Browning of boreal freshwaters coupled to carbon-iron interactions along the aquatic continuum. PLoS One 9 (2), e88104. https://doi.org/10.1371/journal.pone.0088104.

Whitehead, P.G., Wilby, R.L., Battarbee, R.W., Kernan, M., Wade, A.J., 2009. A review of the potential impacts of climate change on surface water quality. Hydrol. Sci. J. 54, 101–123. https://doi.org/10.1623/hysj.54.1.101.

Willén, E., 2001. Phytoplankton and water quality characterization: Experiences from the Swedish large lakes Mälaren, Hjälmaren, Vättern and Vänern. Ambio 30, 529–537. https://doi.org/10.1579/0044-7447-30.8.529.

Winder, M., Schindler, D.E., 2004. Climatic effects on the phenology of lake processes. Glob. Chang. Biol. 10, 1844–1856. https://doi.org/10.1111/j.1365-2486.2004.00849.x.

Yang, Y., Stenger-Kovács, C., Padisák, J., Pettersson, K., 2016. Effects of winter severity on spring phytoplankton development in a temperate lake (Lake Erken, Sweden). Hydrobiologia 780, 47–57. https://doi.org/10.1007/s10750-016-2777-8.

Zibordi, G., Berthon, J.F., Mélin, F., D'Alimonte, D., Kaitala, S., 2009a. Validation of satellite ocean color primary products at optically complex coastal sites: Northern Adriatic Sea, Northern Baltic Proper and Gulf of Finland. Remote Sens. Environ. 113, 2574–2591. https://doi.org/10.1016/j.rse.2009.07.013.

Zibordi, G., Mélin, F., Berthon, J.-F., Holben, B., Slutsker, I., Giles, D., D'Alimonte, D., Vandemark, D., Feng, H., Schuster, G., Fabbri, B.E., Kaitala, S., Seppälä, J., 2009b. AERONET-OC: A network for the validation of ocean color primary products. J. Atmos. Ocean. Technol. 26 (8), 1634–1651. https://doi.org/10.1175/2009JTECHO654.1.

Zibordi, G., Holben, B.N., Talone, M., D'Alimonte, D., Slutsker, I., Giles, D.M., Sorokin, M.G., 2021. Advances in the Ocean Color Component of the Aerosol Robotic Network (AERONET-OC). J. Atmos. Ocean. Technol. 38 (4), 725–746.